

# Implications of QCD radiative corrections on high- $p_T$ Higgs searches

Andrea Banfi<sup>1</sup>, Julián Cancino<sup>2</sup>

<sup>1</sup> Albert-Ludwigs-Universität Freiburg, Physikalisches Institut, D-79104 Freiburg, Germany.

<sup>2</sup> Institute for Theoretical Physics, ETH Zurich, 8093 Zurich, Switzerland.

## Abstract

We discuss the effect of next-to-leading order (NLO) QCD corrections to the Higgsstrahlung process, where the Higgs boson decays to bottom quarks, using a partonic-level fully differential code. First we evaluate the impact of initial- and final-state gluon radiation on the reconstruction of a mass peak with the fat-jet analysis in the boosted regime at the LHC with  $\sqrt{s} = 14$  TeV as proposed in Butterworth et al. (2008) [1]. We then consider the current CMS search strategy for this channel and compare it to the fat-jet procedure at the LHC with  $\sqrt{s} = 8$  TeV. Both studies show that final-state QCD radiation has a sizeable effect and should be taken properly into account.

## 1 Introduction

Although the LHC has started its operations only a couple of years ago and at half the design energy, it has already provided plenty of information on the existence of a Standard Model (SM) Higgs boson. With the  $5 \text{ fb}^{-1}$  luminosity collected with  $\sqrt{s} = 7$  TeV at the end of 2011, ATLAS was able to exclude the presence of a SM Higgs boson in the range  $133 \text{ GeV} < m_H < 230 \text{ GeV}$  and  $260 \text{ GeV} < m_H < 437 \text{ GeV}$  [2], and CMS in the range  $129 \text{ GeV} < m_H < 525 \text{ GeV}$  [3], in both cases at 99% confidence level. Furthermore, adding  $6 \text{ fb}^{-1}$  of the 2012 run at  $\sqrt{s} = 8$  TeV, it has been recently possible to discover a new boson with mass around 125 GeV [4, 5]. It remains to establish whether this boson is indeed the SM Higgs by studying in detail all its decay modes. A light Higgs boson directly produced in gluon-gluon fusion (the process giving the largest cross section) decays predominantly into a  $b\bar{b}$  pair, where the signal is overwhelmed by the huge QCD dijet background. This is why the decay modes that have led to the discovery are those who do not involve hadronic final states, like  $H \rightarrow \gamma\gamma$  [6, 7],  $H \rightarrow WW$  [8, 9] or  $H \rightarrow ZZ$  [10, 11, 12]. Although they are suppressed with respect to the dominant  $b\bar{b}$  mode, it is still possible to extract a signal from the background. There is yet another possibility to exploit the  $b\bar{b}$  decay of the Higgs boson, namely when it is produced in association with a vector boson  $V$  ( $W$  or  $Z$ ): the

Higgsstrahlung process. In this case there are various possibilities to disentangle the signal over the large  $Vb\bar{b}$  background, some of which have been already used at the LHC [13, 14]. Among them, one of the most promising strategies makes use of the fact that at the LHC, especially at  $\sqrt{s} = 14$  TeV, it is possible to produce particles with transverse momenta well above their masses. It is the so-called “boosted” regime, in which one can reconstruct heavy particles decaying hadronically, because their decay products are likely to fall inside one jet with a large radius, a.k.a. *fat jet*. Recent proposals for finding a boosted Higgs boson decaying into a  $b\bar{b}$  pair are based on the investigation of the substructure of each fat jet [1, 15]. Within these approaches the Higgs boson candidate is a multi-jet system which should contain not only the Higgs boson decay products, but also QCD radiation associated to them. It is therefore extremely important to have predictions for the  $VH$  process that implement gluon radiation, both from the initial and final state.

Higher-order corrections to the Higgsstrahlung process, with the Higgs boson decaying into a  $b\bar{b}$  pair, have been known since a long time. NLO corrections to Higgs boson production in association with a vector boson have been computed in Refs. [16, 17, 18] and implemented in the program MCFM [19]. Leading electro-weak corrections are available as well [20] and implemented, together with QCD corrections, in the program HAWK [21]. NNLO results exist for the total cross section [22] for both  $WH$  and  $ZH$  processes, while a fully differential code is available for  $WH$  production only [23]. In all these production codes the decay of the Higgs into a  $b\bar{b}$  pair is implemented at LO only. Concerning decay, NLO corrections for massive bottom quarks have been computed in Ref. [24], while for massless bottom quarks a fully differential calculation is available at NNLO [25]. NLO corrections have been interfaced to parton showers in the MC@NLO framework in Ref. [26]. Furthermore, starting from version 2.5, Herwig++ [27] implements NLO corrections to Higgs boson production [28] and Higgs boson decay, both matched independently to parton shower.

Investigating the effect of NLO QCD corrections to both production and decay on present and future Higgs searches is the aim of the present Letter. We do this in the case of Higgs boson production in association with a  $W$  boson. Since to our knowledge no fixed-order program implements NLO QCD corrections to both Higgs boson production and decay, we have decided to construct a new code based on the already available matrix elements. Having our own fully differential code give us the opportunity to study NLO QCD corrections to production and decay in a completely separate way. We stick to a fixed-order calculation since its outcome can be interpreted more easily than the corresponding one from Monte Carlo event generators. The latter in fact supplements the hard matrix element with soft and/or collinear emissions, which can induce modifications on pure NLO effects. However, although we do not present any prediction obtained with Monte Carlo event generators, we will discuss how potential instabilities of fixed-order calculations can be removed either with all-order QCD resummation or with parton shower Monte Carlo’s.

We now describe the details of our calculation. Denoting by  $d\sigma_{pp\rightarrow WH}$  the differential cross section for  $WH$  production and by  $d\Gamma_{H\rightarrow b\bar{b}}$  the differential decay rate for a Higgs

boson decaying into a  $b\bar{b}$  pair we have the perturbative expansions

$$d\sigma_{pp \rightarrow WH} = d\sigma_{pp \rightarrow WH}^{(0)} + d\sigma_{pp \rightarrow WH}^{(1)}, \quad d\Gamma_{H \rightarrow b\bar{b}} = d\Gamma_{H \rightarrow b\bar{b}}^{(0)} + d\Gamma_{H \rightarrow b\bar{b}}^{(1)}, \quad (1.1)$$

where  $d\sigma_{pp \rightarrow WH}^{(1)}$  is of relative order  $\alpha_s$  with respect to  $d\sigma_{pp \rightarrow WH}^{(0)}$  (and similarly  $d\Gamma_{H \rightarrow b\bar{b}}^{(1)}$  with respect to  $d\Gamma_{H \rightarrow b\bar{b}}^{(0)}$ ). Using the narrow width approximation, which is reasonable for a light SM Higgs, we can combine NLO corrections to production and decay as follows

$$d\sigma_{pp \rightarrow (H \rightarrow b\bar{b})W} = \left( d\sigma_{pp \rightarrow WH}^{(0)} \times \frac{d\Gamma_{H \rightarrow b\bar{b}}^{(0)} + d\Gamma_{H \rightarrow b\bar{b}}^{(1)}}{\Gamma_{H \rightarrow b\bar{b}}^{(0)} + \Gamma_{H \rightarrow b\bar{b}}^{(1)}} + d\sigma_{pp \rightarrow WH}^{(1)} \times \frac{d\Gamma_{H \rightarrow b\bar{b}}^{(0)}}{\Gamma_{H \rightarrow b\bar{b}}^{(0)}} \right) \times \text{Br}(H \rightarrow b\bar{b}), \quad (1.2)$$

where  $\Gamma_{H \rightarrow b\bar{b}}^{(0)}$  is the LO total  $H \rightarrow b\bar{b}$  decay rate,  $\Gamma_{H \rightarrow b\bar{b}}^{(1)}$  the corresponding NLO correction and  $\text{Br}(H \rightarrow b\bar{b})$  is the branching ratio for the decay  $H \rightarrow b\bar{b}$ . Before describing the phenomenology we briefly give some details of the calculation. To handle infrared divergences we use a fully local subtraction method both for production and decay. We first compute real and virtual matrix elements in  $4 - 2\epsilon$  dimensions. We then suitably parametrise the phase space for the emission of a single real gluon, expand each denominator occurring in the real matrix element in powers of  $\epsilon$ , and cancel all the resulting  $1/\epsilon^2$  and  $1/\epsilon$  poles point by point in phase space either against virtual corrections, or against the collinear counterterm provided by the  $\overline{\text{MS}}$  factorisation scheme. For the production process, we use, depending on the computation order, the LO or NLO MSTW2008 parton densities [29] interfaced through LHAPDF [30], the latter corresponding to  $\alpha_s(M_Z) = 0.120179$ , which is the value we use for NLO corrections. We consider both  $W^+$  and  $W^-$  production, keeping the full spin correlations when letting them decay into a lepton and a neutrino. Concerning Higgs boson decay, all matrix elements for  $H \rightarrow b\bar{b}$  are computed for massive bottom quarks, using the on-shell renormalisation scheme with a pole mass  $m_b = 4.24 \text{ GeV}$ . We have checked that our production code agrees with MCFM, and our total decay rate reproduces the NLO result of Ref. [24]. Furthermore, in the following we will consider the production of a Standard Model Higgs boson of mass  $m_H = 125 \text{ GeV}$ , with  $\text{Br}(H \rightarrow b\bar{b}) = 0.578$  taken from Refs. [31, 32, 33].<sup>1</sup>

## 2 NLO corrections to Higgs searches with the fat-jet method

A natural place to look for a boosted Higgs boson is the LHC with  $\sqrt{s} = 14 \text{ TeV}$  at high luminosity, where one has the possibility to cut on a high-transverse momentum Higgs boson, and still have a number of events that make it possible to significantly distinguish the signal from the background. Therefore, we first give theoretical predictions for observables

---

<sup>1</sup>In fact, since we will be concerned mainly on  $K$ -factors and shapes of distributions, the actual value of  $\text{Br}(H \rightarrow b\bar{b})$  will not be relevant for the main issues discussed in the Letter.

that are of use at the LHC with  $\sqrt{s} = 14$  TeV when searching for a boosted Higgs boson associated to a  $W$  boson, using the strategy of Ref. [1]. In the following we describe the set of kinematical cuts we employ for our theoretical analysis. First of all, we put some basic constraints on the decay products of the  $W$  boson, namely that the charged lepton has a transverse momentum  $p_T^l > 30$  GeV and a pseudorapidity  $|\eta| < 2.5$ , and that the total missing transverse momentum fulfils  $p_T^{\text{miss}} > 30$  GeV. We then require that the reconstructed  $W$  boson have large transverse momentum  $p_T^W > 210$  GeV. This value is approximately equal to the minimum transverse momentum that a boosted Higgs boson recoiling against a  $W$  boson must have, at tree level, so that the  $b\bar{b}$  pair resulting from its decay falls into a cone of radius  $R = 1.2$ . The latter is the value of jet radius  $R$  considered in Ref. [1]. Specifically, a Higgs boson decaying into a  $b\bar{b}$  pair is searched for by clustering each event into fat jets using the Cambridge/Aachen algorithm [34, 35] from the software package FastJet [36] with  $R = 1.2$ , and examining the substructure of each jet to see if it contains the Higgs boson decay products. Once we have identified a fat jet, in order to establish whether it can be considered a Higgs candidate, we follow the procedure proposed in Ref. [1], which we briefly recall:

1. we undo the last clustering inside the fat jet  $j$ , thus identifying two subjets  $j_1$  and  $j_2$  ordered according to their invariant mass,  $m_{j_1}^2 > m_{j_2}^2$ ;
2. we require a significant mass drop  $m_{j_1}^2 < \mu m_j^2$  and impose  $\max\{p_{T,1}^2, p_{T,2}^2\} \Delta R_{j_1, j_2}^2 > y_{\text{cut}} m_j^2$ , in order to suppress asymmetric splittings.

If both conditions are fulfilled then  $j$  is a candidate Higgs jet and the procedure terminates. Otherwise  $j = j_1$  and we go back to step 1. The fat jet is then kept as a Higgs candidate only if both  $j_1$  and  $j_2$  have  $b$ -tags. Finally, again following Ref. [1], one should apply a filtering procedure, which consists in reclustering the candidate Higgs jet with a radius  $R_{\text{filt}} < R$ , and then choosing the candidate Higgs mass as the invariant mass of the hardest (i.e. with the highest  $p_T$ )  $n_{\text{filt}}$  subjets. Since our calculation is pure NLO for both production and decay, a fat jet will contain at most three subjets. As suggested in Ref. [1], we choose  $n_{\text{filt}} = 3$ , and therefore we can skip the filtering step at this stage. However the full procedure has been programmed in our numerical code, so that it can be used when NNLO corrections to both production and decay will be implemented.

The first relevant observable we consider is the transverse momentum  $p_{T,j}$  of the candidate Higgs jet. In particular, we wish to perform an analogous study as in Ref. [23], including NLO corrections to both Higgs boson production and decay. As in Ref. [23], we require the candidate Higgs jet to be the one with the highest transverse momentum and to be central,  $|\eta_j| < 2.5$ . In Fig. 1 we show plots for the fat-jet  $p_T$ -spectrum corresponding to two different event selection procedures. In the first case no constraint is imposed on any extra jet, whilst in the second case we impose a jet-veto condition, requiring that there are no further jets with  $p_T > p_{T,\text{veto}} = 30$  GeV and  $|\eta| < \eta_{\text{veto}} = 3$  (again according to what is done in Ref. [1]). The perturbative stability of our predictions is investigated by simultaneous variation of renormalisation and factorisation scales for the production process by a factor of two around  $\mu_R^{(p)} = \mu_F^{(p)} = m_H + m_W$ . Since we know from the study of Ref. [37]

that, for the fat-jet analysis described above, no infrared problems are expected from QCD corrections to the decay process, we have decided to fix the renormalisation scale for the decay at  $\mu_R^{(d)} = m_H$ .

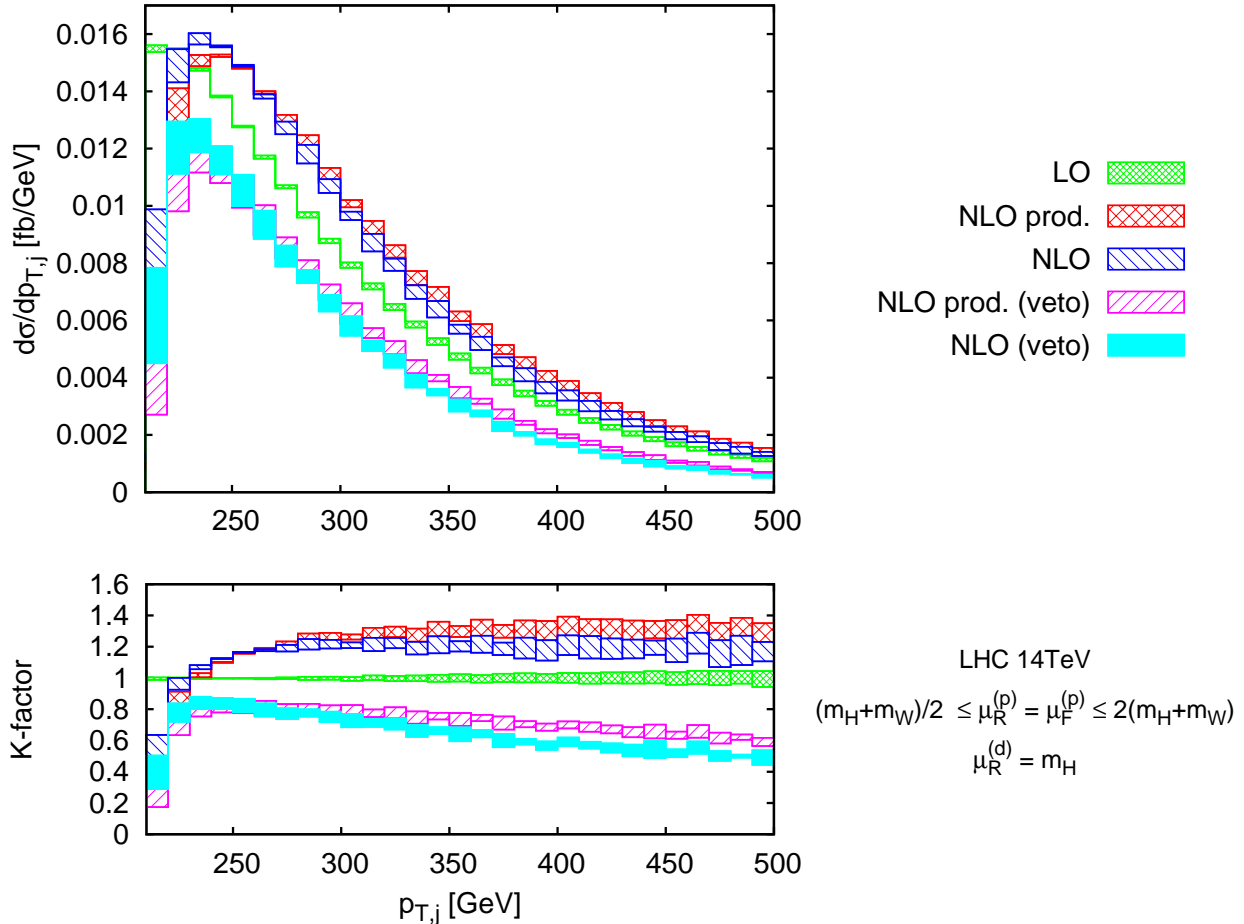


Figure 1: The transverse momentum distribution of the candidate Higgs fat jet at the LHC with  $\sqrt{s} = 14$  TeV, corresponding to the kinematical cuts described in the text. (For interpretation of the references to colour, the reader is referred to the web version of this Letter.)

At LO the distributions with and without an extra-jet veto obviously coincide. On the contrary, as observed already in Ref. [23], there are substantial differences for NLO distributions. Without a veto on an extra jet, if one excludes the lowest  $p_T$ -bin, NLO corrections to production are positive, giving roughly a constant  $K$ -factor of about 1.3 at large  $p_{T,j}$ . The addition of NLO corrections to decay does not alter significantly this  $K$ -factor, reducing it to 1.2 (see Fig. 1, red and dark-blue bands). The fact that the  $K$ -factor is only slightly decreased when adding NLO corrections to decay suggests that the observable we consider is sufficiently inclusive with respect to extra gluon radiation from the  $b\bar{b}$  system. In other words, in the boosted regime we are considering, final-state QCD

	LO	NLO (prod.)	NLO
$\sigma_{\text{inc}}$ [fb]	$1.53^{+0.02}_{-0.03}$	$1.87^{+0.05}_{-0.05}$	$1.80^{+0.06}_{-0.07}$
$\sigma_{0\text{-jet}}$ [fb]	$1.53^{+0.02}_{-0.03}$	$1.19^{+0.04}_{-0.06}$	$1.12^{+0.06}_{-0.08}$

Table 1: Cross section for Higgs boson production in association to a high- $p_T$   $W$  boson selected according to the cuts described in the main text, for  $230 \text{ GeV} < p_{T,j} < 500 \text{ GeV}$ , with ( $\sigma_{0\text{-jet}}$ ) and without ( $\sigma_{\text{inc}}$ ) a veto on an extra jet. The intervals are obtained by varying the scales for production and decay by a factor two around the central values described in the text.

radiation is well contained inside the fat jet, and therefore we observe no large virtual corrections unbalanced by real radiation. After imposing the jet veto, NLO corrections become negative, and increase in size when the jet transverse momentum increases. This is due to virtual contributions that do not cancel fully against initial-state real radiation, giving a (negative) logarithmic left-over as large as  $\alpha_s \ln^2(p_{T,j}/p_{T,\text{veto}})$ .<sup>2</sup> We observe that, also in this case, the addition of NLO corrections to decay causes only a mild reduction of the  $K$ -factor, around 10% and roughly constant over the whole fat-jet  $p_T$ -range (see Fig. 1, purple and light-blue bands). An important remark is in order concerning the behaviour of the fat-jet  $p_T$ -spectrum in the lowest  $p_T$ -bin. There one notices a significant decrease in the cross section in going from LO to NLO, as well as a larger variation when changing renormalisation and factorisation scales. This bin corresponds in fact to the situation in which one imposes symmetric  $p_T$  cuts on both the Higgs boson and the  $W$  boson. As observed in Refs. [42, 43] and explained in Ref. [44], symmetric cuts can cause instabilities in the QCD perturbative series. However [44], such instabilities could be removed by performing a resummation of large logarithms appearing in the distribution in the transverse momentum of the  $HW$  system. The physics underlying such resummation is implemented in all parton shower Monte Carlo's, which should then be used for Higgs searches including the symmetric-cut region. Performing such a resummation is beyond the scope of this work. Therefore, we restrict our subsequent analyses to the asymmetric-cut region  $p_{T,j} > 230 \text{ GeV}$ , where our fixed-order predictions seem to be reliable. Finally, since our code is not public yet, in Table 1 we report an example of the cross sections we obtain for the integrated  $p_T$  spectrum for  $\mu_R^{(p)} = \mu_F^{(p)} = m_H + m_W$  and of  $\mu_R^{(d)} = m_H$ , together with the corresponding renormalisation and factorisation scale uncertainties.

From the plots in Fig. 1 it seems that the net effect of QCD corrections to Higgs boson decay is just that of reducing the production rate of a candidate Higgs fat jet. However, the fat jet considered there can have an arbitrary invariant mass, whilst in general one measures the fat-jet invariant mass distribution, given a set of kinematical cuts, and looks for a mass peak. Therefore, it is useful to investigate the impact of NLO corrections to Higgs boson

---

<sup>2</sup>Note that double logarithmic contributions  $\alpha_s \ln^2(p_{T,j}/p_{T,\text{veto}})$  occur in this case because, as explained in Ref. [38],  $\ln(p_{T,j}/p_{T,\text{veto}})$  is smaller than the maximum rapidity  $\eta_{\text{veto}}$  available for the additional jets. These logarithms could in principle be resummed at all orders with the methods developed in Refs. [38, 39, 40, 41].

production and decay over the reconstruction of a mass peak based on the fat-jet analysis described at the beginning of this section. At NLO there are two effects that can spoil this reconstruction, both triggered by gluon radiation. The first is the emission of a parton from the initial state that is subsequently clustered within the fat jet. The second is the loss of gluon radiation from the  $b\bar{b}$  pair originating from the decay of the Higgs boson. Both effects are studied through the plots in Fig. 2, showing the differential distribution  $d\sigma/dm_j$  in the invariant mass of the fat jet, for  $\mu_R^{(p)} = \mu_F^{(p)} = m_H + m_W$  and  $\mu_R^{(d)} = m_H$ . The first

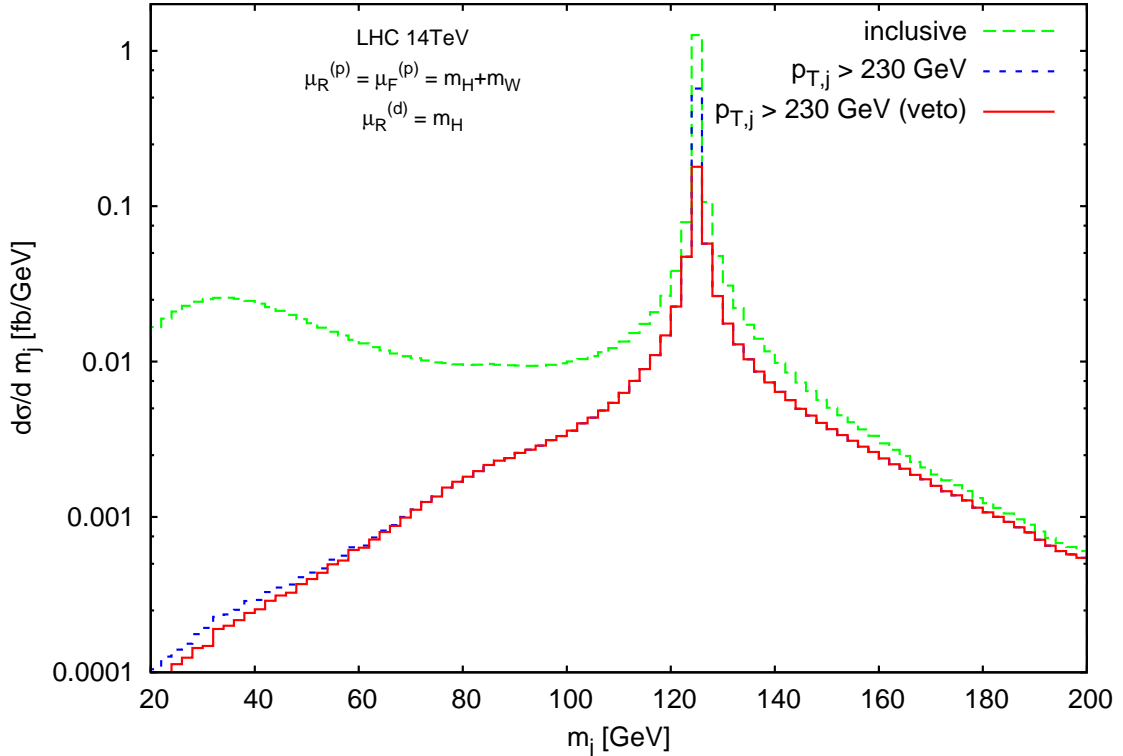


Figure 2: The distribution in the invariant mass of the candidate Higgs jet, without any kinematical cuts (green, dashed, labelled “inclusive”), fully inclusive with respect to all other jets (blue, dashed, labelled “ $p_{T,j} > 230$  GeV”), and with a jet-veto condition (red, solid, labelled “ $p_{T,j} > 230$  GeV (veto)”). All curves correspond to  $\mu_R^{(p)} = \mu_F^{(p)} = m_H + m_W$  for Higgs boson production and  $\mu_R^{(d)} = m_H$  for its decay.

NLO curve in Fig. 2 (green, dashed) corresponds to the fully inclusive situation in which the only selection requirement is that there is a candidate Higgs jet, with no cut whatsoever on the jet transverse momentum. This curve is shown to illustrate how the fat-jet selection technique works in practice. We first observe that the fat-jet method is pretty robust under radiative corrections, in that, even without requiring a high- $p_T$   $W$  boson, only around 30% of candidate Higgs events fall outside the mass window  $110 \text{ GeV} < m_j < 140 \text{ GeV}$  (a typical bin size for boosted Higgs searches at the LHC, see [13]). The region to the right of the peak corresponds to situations in which initial-state radiation is clustered inside the fat jet,

thus artificially increasing the invariant mass of the latter. To the left of the peak we see a long tail corresponding to events in which a gluon emitted from the  $b\bar{b}$  system originating from Higgs boson decay escapes the fat jet. This effect is entirely due to NLO corrections to Higgs boson decay, and its contribution to degrading the resolution of the mass peak is comparable to that coming from NLO corrections to Higgs boson production. In fact, most events outside the mass window  $110 \text{ GeV} < m_j < 140 \text{ GeV}$  have  $m_j < 110 \text{ GeV}$ . These events extend down to  $m_j = 2m_b$ , corresponding to the situation in which the  $b\bar{b}$  pair recoils against a hard gluon. The other two curves correspond to events passing the same kinematical cuts as in Fig. 1, and with an additional cut on the fat-jet transverse momentum  $p_{T,j} > 230 \text{ GeV}$ . We first observe that this cut reduces considerably the fraction of events with  $m_j < 110 \text{ GeV}$  which is around 10% both with and without the jet veto. A further remark is in order concerning the curve (solid, red) obtained by imposing the additional constraint of vetoing all extra jets with  $p_T > 30 \text{ GeV}$  and rapidity  $|\eta| < 3$ . In this case, as expected from the study of Ref. [23] and Fig. 1, the peak height is reduced due the suppression of real emission and the dominance of negative uncanceled virtual corrections. Among the effects of the jet veto there is also that of eliminating events in which a gluon emitted by the  $b\bar{b}$  system escapes the fat jet. For the red solid curve this is visible in the figure for  $m_j < 60 \text{ GeV}$  and has a negligible impact on the resolution of the mass peak. We finally remark that the fact that the mass peak survives depends crucially on both the jet-veto condition and the procedure used to identify a candidate Higgs jet. We have observed that decreasing  $p_{T,\text{veto}}$  can lower the number of selected events in such a way that a peak is not visible any more. The same remark holds for alternative procedures for defining a candidate Higgs jet, which need to be tested against final-state QCD radiation as well. An example of how the latter can affect significantly the outcome of a Higgs search analysis is discussed in the next section.

### 3 Higgs searches at the LHC with $\sqrt{s} = 8 \text{ TeV}$

With the current LHC energy, CMS is searching for a high- $p_T$  Higgs radiated off a vector boson. They do not perform a full fat-jet analysis, but instead use a simplified procedure aimed at identifying a boosted hadronic system that could be considered as a Higgs candidate [13]. Here is a summary of the CMS analysis. First, they impose cuts on the decay products of the  $W$  boson. For a  $W$  boson decaying into a muon and its associated neutrino (the case we consider in the following), they require  $p_T^\mu > 20 \text{ GeV}$  and  $|\eta| < 2.4$ , together with a constraint on the missing transverse energy  $p_T^{\text{miss}} > 35 \text{ GeV}$ . The Higgs candidate is a dijet system consisting of two central ( $|\eta| < 2.5$ )  $b$ -tagged jets with  $p_T > 30 \text{ GeV}$ , reconstructed with the anti- $k_t$  algorithm [45] with  $R = 0.5$ . Then, high- $p_T$  events are selected by imposing a cut both on the transverse momentum of the reconstructed  $W$  boson  $p_T^W > 160 \text{ GeV}$  and on that of the dijet system  $p_{T,j} > 165 \text{ GeV}$ , and requiring the latter to be central ( $|\eta_j| < 2.5$ ). Finally, the  $W$  boson and the Higgs candidate are required to be almost back-to-back in the transverse plane, by imposing  $\Delta\phi_{W,j} \equiv |\phi_W - \phi_j| > 3$ , and no extra jets are allowed with  $p_T > 20 \text{ GeV}$  and  $|\eta| < 2.4$ .

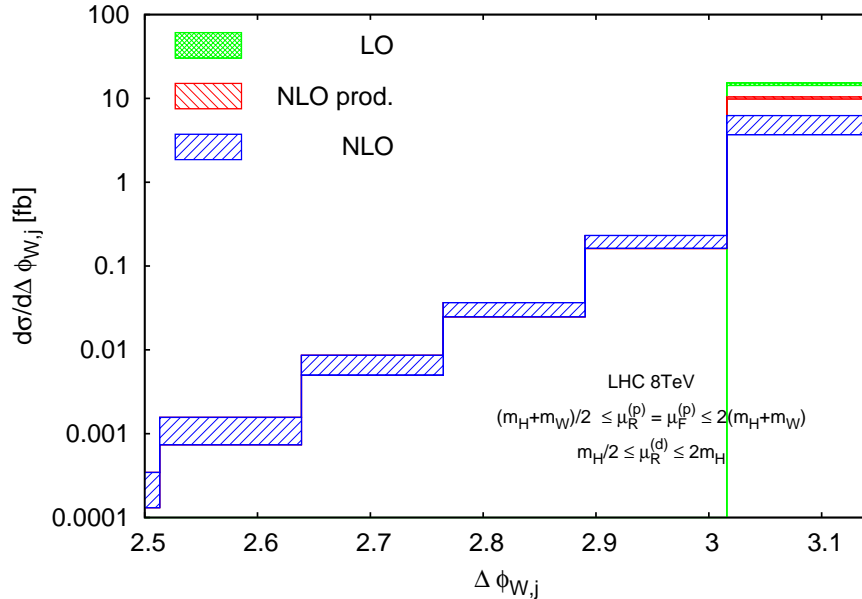


Figure 3: The differential distribution in the azimuthal angle  $\Delta\phi_{W,j}$  between the reconstructed  $W$  boson and the candidate Higgs jet, corresponding to the selection cuts described in the text.

Among these conditions, the requirement on  $\Delta\phi_{W,j}$ , is particularly sensitive to initial-state radiation, in particular soft and collinear gluon emissions along the beam. We wish therefore to investigate if our predictions for the  $\Delta\phi_{W,j}$  distribution are stable against higher-order corrections. We do this via simultaneous variations of renormalisation and factorisation scales for the production process around  $\mu_R^{(p)} = \mu_F^{(p)} = m_H + m_W$ , and independent variation of the renormalisation scale for the decay around  $\mu_R^{(d)} = m_H$ . Fig. 3 shows the  $\Delta\phi_{W,j}$  distribution, obtained after imposing the cuts described above. First of all, one notices that most events are concentrated in the bin  $\Delta\phi_{W,j} > 3$ , so that we expect that bin to be wide enough to ensure a sufficiently inclusive cancellation of large real and virtual corrections arising from the region close to  $\Delta\phi_{W,j} = \pi$ . This is confirmed by the fact that, if one considers production only (the histogram labelled “NLO prod.”), the  $K$ -factor we observe in that bin is moderate (around 0.8). Indeed, the cut on  $\Delta\phi_{W,j}$  is only one of the effects that are responsible for such  $K$ -factor, the others being the cut on the jet  $p_T$  and the jet-veto condition, which can also put constraints on initial-state radiation. We remark that, if the constraint on  $\Delta\phi_{W,j}$  were moved closer to  $\pi$  while keeping all other cuts fixed, one would expect large logarithmic contributions  $\alpha_s^n \ln^m(\pi - \Delta\phi_{W,j})$  arising from multiple initial-state soft-collinear emissions. These could be resummed, either analytically, or using Monte Carlo event generators. When adding final-state radiation, one observes that the height of the distribution in the rightmost bin is further depleted. However, due to the fact that, for  $\Delta\phi_{W,j} < 3$  all NLO distributions basically coincide, this depletion cannot be ascribed to a restriction on final-state radiation imposed indirectly through the cut on  $\Delta\phi_{W,j}$ . The reduction of the cross section is mainly due to the loss of QCD radiation from

the  $b\bar{b}$  system. Due to the jet-veto condition, any gluon that is not clustered inside the two  $b$ -jets that constitute the Higgs candidate is likely to be soft, and therefore  $\Delta\phi_{W,j}$  will be close to  $\pi$ . It is this restriction on final-state radiation that causes an imbalance between real and virtual corrections, giving a large negative contribution. A further source of large virtual corrections, which contribute significantly to the size of the observed  $K$ -factor, is the presence of a term  $\alpha_s \ln(m_b/m_H)$  in the virtual corrections, coming from the on-shell renormalisation of the coupling of the  $b$  quark to the Higgs. To investigate the impact of this term, we use a different prescription to combine NLO corrections to production and decay, by strictly expanding Eq. (1.2) at order  $\alpha_s$ :

$$d\sigma_{pp \rightarrow (H \rightarrow b\bar{b})W}^{\text{exp}} = \left\{ d\sigma_{pp \rightarrow WH}^{(0)} \times \left[ \frac{d\Gamma_{H \rightarrow b\bar{b}}^{(0)}}{\Gamma_{H \rightarrow b\bar{b}}^{(0)}} \left( 1 - \frac{\Gamma_{H \rightarrow b\bar{b}}^{(1)}}{\Gamma_{H \rightarrow b\bar{b}}^{(0)}} \right) + \frac{d\Gamma_{H \rightarrow b\bar{b}}^{(1)}}{\Gamma_{H \rightarrow b\bar{b}}^{(0)}} \right] + d\sigma_{pp \rightarrow WH}^{(1)} \times \frac{d\Gamma_{H \rightarrow b\bar{b}}^{(0)}}{\Gamma_{H \rightarrow b\bar{b}}^{(0)}} \right\} \times \text{Br}(H \rightarrow b\bar{b}). \quad (3.1)$$

We see that the curve corresponding to this last prescription (purple, labelled ‘‘NLO exp.’’) is significantly higher than the curve corresponding to Eq. (1.2) (blue, labelled ‘‘NLO’’). The difference between the two prescriptions can be understood as an indication on the convergence of perturbation theory. In this respect, we have checked that all the results we have obtained in the previous section using the fat-jet procedure are, within scale uncertainties, insensitive to a change of prescription, thus indicating that this procedure is inclusive enough with respect to final-state radiation to ensure good convergence of the perturbative expansion. In the following, whenever relevant, we will use both prescriptions.

We now proceed by presenting the distributions studied in the previous section, this time relative to the candidate Higgs selected according to the CMS procedure, and for LHC at  $\sqrt{s} = 8 \text{ TeV}$ .<sup>3</sup> For the mass distribution, we will also compare the mass spectrum corresponding to the CMS analysis with that obtained with the fat-jet analysis described at the beginning of section 2. In this case  $m_j$  will label the invariant mass of the fat jet.

Fig. 4 contains distributions in the transverse momentum  $p_{T,j}$  of the candidate Higgs dijet system. Each band corresponds to a simultaneous variation of renormalisation and factorisation scale by a factor of two around  $\mu_R^{(p)} = \mu_F^{(p)} = m_H + m_W$  in the production process, while renormalisation scale for the decay is kept fixed at  $\mu_R^{(d)} = m_H$ . If one does not include NLO corrections to decay, one observes a 20% reduction in the cross section with respect to LO. This reduction is driven mainly by the jet-veto condition, and as expected gets more important as the dijet transverse momentum increases. The inclusion of NLO corrections to Higgs boson decay causes a further decrease of the cross section. We interpret this result as a sizable loss of QCD final-state radiation by the two jets that constitute the Higgs candidate system, likely due to the fact that the  $b$  jets have a small radius and the typical perturbative jet  $p_T$ -loss increases with decreasing radius, as explained in Ref. [46], and the lost radiation undergoes a jet-veto constraint. This in turns causes a poor

---

<sup>3</sup>We have checked that our considerations do not change in the case of LHC at  $\sqrt{s} = 7 \text{ TeV}$ .

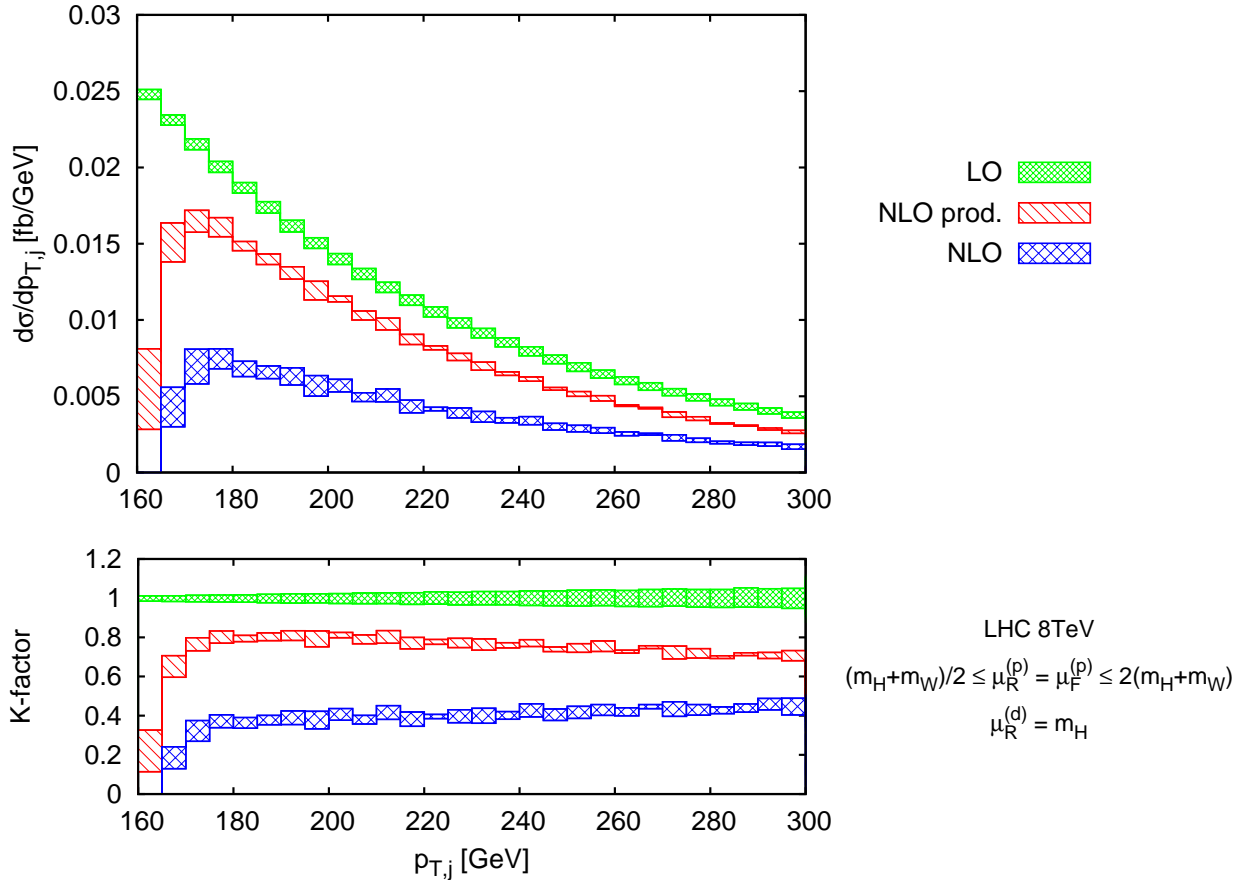


Figure 4: The distribution in the transverse momentum  $p_{T,j}$  of the candidate Higgs dijet system, corresponding to the selection cuts described in the text.

convergence of the perturbative series, as one observes by comparing the “NLO” and “NLO exp.” curves. We have checked that this does not happen if one performs a fat-jet analysis with the same parameters as in Sec. 2, where one observes instead a  $K$ -factor of around 0.6 for  $p_{T,j} > 250$  GeV, although in this case the  $p_{T,j}$  distribution drops abruptly, as expected, for  $p_{T,j} < 200$  GeV. We have also checked that for larger  $p_T$  values ( $p_{T,j} > 350$  GeV) the CMS and fat-jet procedure give comparable  $p_{T,j}$  spectra. Another remark concerns the first bin ( $160 \text{ GeV} < p_{T,j} < 165 \text{ GeV}$ ), where the distribution is unstable against scale variations (it becomes even negative if one includes corrections to Higgs boson decay), again due to the fact that this bin corresponds to symmetric transverse momentum cuts, in which the  $W$  boson and the  $b$ -dijet system recoil against a soft-collinear gluon. This bin is not included in the CMS analysis, and will not be considered in all our subsequent studies.

We then present in Fig. 5 the distribution in the invariant mass of the candidate Higgs system  $d\sigma/dm_j$ . We consider here four distributions, the first (solid, red) obtained with the CMS selection procedure, the second (dashed, blue) corresponding to the fat-jet selection procedure explained at the beginning of Sec. 2, with the same selection cuts as CMS

for the leptons, the  $W$  boson and the candidate Higgs system, the third (dashed, green) corresponding to the CMS procedure but where only NLO corrections to the production process are considered, and the fourth (dotted, purple) again corresponding the CMS procedure and obtained using Eq. (3.1). From the plots we see that the mass distribution

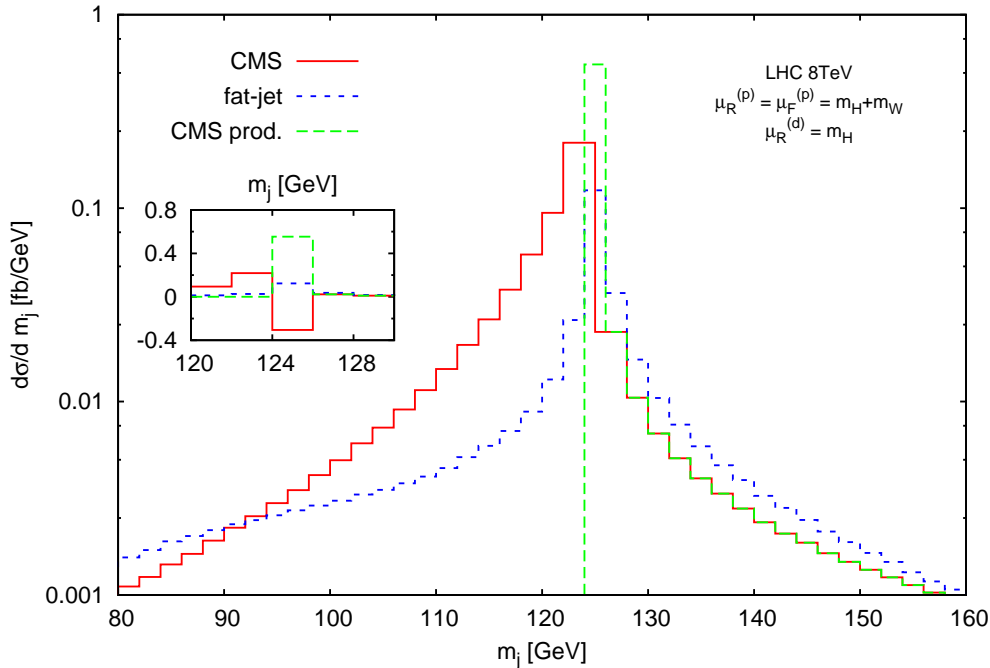


Figure 5: The distribution in the invariant mass  $m_j$  of the candidate Higgs jet obtained with the procedure adopted by CMS, with and without NLO corrections to Higgs decay, and with the fat-jet procedure described in Sec. 2.

resulting from the CMS procedure (red, solid), catches more candidate Higgs events than the fat-jet one, as expected due to the lower  $p_T$ -cut on the selected  $b$ -jets. However, the mass distribution does not display a mass peak in the expected position. In fact the value of the distribution at  $m_j = 125$  GeV is negative (see inset plot of Fig. 5) if one uses Eq. (1.2), and only slightly positive if one uses instead Eq. (3.1) (the purple dotted curve labelled “CMS exp.”). Regardless of the actual value of the distribution at  $m_j = 125$  GeV, this clearly indicates that radiation from the  $b\bar{b}$  pair originating from Higgs boson decay is not naturally included in the candidate Higgs system. On the contrary, the fat-jet procedure (blue, dashed) gives correctly a peak at  $m_j = 125$  GeV, although with a reduced height with respect to that of the shifted peak resulting from the CMS procedure. This result does not change if one uses the alternative prescription of Eq. (3.1). The third curve (green, dashed) shows the mass distribution obtained by considering NLO corrections to production only. We notice that the peak is in the expected position, with a height that is roughly five times larger than that of the peak corresponding to the fat-jet procedure. In this respect, we remark that the parameters we have chosen for the fat-jet analysis are identical to those of Sec. 2. In principle one should redetermine them after a full simulation

of signal and background, including parton shower effects (for instance using the recent developments of Ref. [28]). This goes beyond the scope of this work.

## 4 Conclusions

We have implemented NLO corrections to Higgs boson production in association with leptonically decaying  $W$  boson, and to its subsequent decay into a  $b\bar{b}$  pair, in a numerical code that returns weighted events, fully differential in the decay products of the Higgs boson and of the  $W$  boson. We have then looked at how NLO QCD corrections to Higgs boson decay affect various observables that are relevant for Higgs searches at the LHC. In particular we have analysed two different experimental setups, one with  $\sqrt{s} = 14$  TeV and the other with  $\sqrt{s} = 8$  TeV. In the first case the Higgs boson is produced in a boosted regime, with its transverse momentum larger than its mass, and detected using the fat-jet technique proposed in Ref. [1]. With our study in Section 2 we assess that the Higgs candidate obtained with the fat-jet procedure is stable against radiative corrections. Its mass distribution is peaked at the expected value of the Higgs boson mass, and the resolution of the peak is reasonably good (see Fig. 2). We remark that the height of the peak is sensitive to the jet-veto condition that one imposes on any jet besides the candidate Higgs fat jet, the stronger the veto the stronger the suppression of the peak. In our case the height of the peak obtained after imposing a jet-veto condition is roughly a third of that we get if we are fully inclusive with respect to all jets. The second experimental setup we have considered corresponds to what is done at the moment by the CMS experiment, but for the LHC current energy  $\sqrt{s} = 8$  TeV. CMS chooses configurations in which both the Higgs boson and the  $W$  boson have high transverse momentum. Then they do not perform a full fat-jet analysis, but rather consider as a Higgs candidate a system of two  $b$ -jets satisfying a set of transverse momentum and rapidity cuts. Again we have checked how relevant distributions are influenced by QCD corrections to Higgs boson decay. We have found that such corrections have a huge impact both on the candidate Higgs transverse momentum spectrum and on its invariant mass distribution. In particular, for the latter it turns out that the effect of an extra jet-veto and the loss of QCD radiation from the  $b\bar{b}$  system give a displacement of the mass peak from its expected position, with a poor peak resolution. This suggests an instability of the CMS procedure against radiative corrections, and reveals how important it is to have NLO information on the Higgs boson decay as well. We remark that the use of a parton shower event generator will give a smoother mass distribution, but will not significantly improve the mass resolution of the peak, which is mainly affected by the large  $p_T$  loss of the selected  $b$ -jets. For comparison we have also studied the jet-mass distribution for a candidate Higgs jet obtained with the same fat-jet procedure considered for the LHC at  $\sqrt{s} = 14$  TeV. Also in this case the procedure seems stable under radiative corrections, and we are able to reconstruct a mass peak in the expected position.

The study we have performed gives some new information on the impact of higher-order corrections on the Higgsstrahlung process, but is far from conclusive. More studies are needed both to improve the accuracy of the calculation, including for instance NNLO

corrections to both production and decay, and to devise procedures to cure the instabilities we have found in our analysis. We aim to address both issues in the near future.

**Acknowledgements** We are grateful to Babis Anastasiou for suggesting us to look into this problem, and for support and illuminating discussions while this work was being performed. We also thank Gavin Salam for a careful reading of the manuscript and insightful comments and suggestions. AB would like also to thank Stefan Gieseke and Keith Hamilton for discussions on Herwig++, and Stefan Dittmaier for pointing out relevant references. The work of J.C. is supported by the ERC Starting Grant for the project “IterQCD” and the Swiss National Foundation under the contract SNF 200020-126632. Part of this work was performed while A.B. was at ETH Zurich.

## References

- [1] J. M. Butterworth, A. R. Davison, M. Rubin, and G. P. Salam, *Phys.Rev.Lett.* **100** (2008) 242001, [[arXiv:0802.2470](#)].
- [2] ATLAS Collaboration, G. Aad *et al.*, *Phys.Lett.* **B710** (2012) 49–66, [[arXiv:1202.1408](#)].
- [3] CMS Collaboration, S. Chatrchyan *et al.*, *Phys.Lett.* **B710** (2012) 26–48, [[arXiv:1202.1488](#)].
- [4] ATLAS Collaboration, G. Aad *et al.*, *Phys.Lett.B* (2012) [[arXiv:1207.7214](#)].
- [5] CMS Collaboration, S. Chatrchyan *et al.*, *Phys.Lett.B* (2012) [[arXiv:1207.7235](#)].
- [6] ATLAS Collaboration, G. Aad *et al.*, *Phys.Rev.Lett.* **108** (2012) 111803, [[arXiv:1202.1414](#)].
- [7] CMS Collaboration, S. Chatrchyan *et al.*, *Phys.Lett.* **B710** (2012) 403–425, [[arXiv:1202.1487](#)].
- [8] ATLAS Collaboration, G. Aad *et al.*, [arXiv:1206.0756](#).
- [9] CMS Collaboration, S. Chatrchyan *et al.*, *Phys.Lett.* **B710** (2012) 91–113, [[arXiv:1202.1489](#)].
- [10] ATLAS Collaboration, G. Aad *et al.*, *Phys.Lett.* **B710** (2012) 383–402, [[arXiv:1202.1415](#)].
- [11] CMS Collaboration, S. Chatrchyan *et al.*, *Phys.Rev.Lett.* **108** (2012) 111804, [[arXiv:1202.1997](#)].
- [12] CMS Collaboration, S. Chatrchyan *et al.*, *JHEP* **1203** (2012) 040, [[arXiv:1202.3478](#)].

- [13] CMS Collaboration, S. Chatrchyan *et al.*, *Phys.Lett.* **B710** (2012) 284–306, [[arXiv:1202.4195](#)].
- [14] ATLAS Collaboration, G. Aad *et al.*, [arXiv:1207.0210](#).
- [15] A. Abdesselam, E. B. Kuutmann, U. Bitenc, G. Brooijmans, J. Butterworth, *et al.*, *Eur.Phys.J.* **C71** (2011) 1661, [[arXiv:1012.5412](#)].
- [16] R. Hamberg, W. van Neerven, and T. Matsuura, *Nucl.Phys.* **B359** (1991) 343–405.
- [17] H. Baer, B. Bailey, and J. Owens, *Phys.Rev.* **D47** (1993) 2730–2734.
- [18] J. Ohnemus and W. J. Stirling, *Phys.Rev.* **D47** (1993) 2722–2729.
- [19] J. Campbell and K. Ellis, <http://mcfm.fnal.gov>.
- [20] M. Ciccolini, S. Dittmaier, and M. Kramer, *Phys.Rev.* **D68** (2003) 073003, [[hep-ph/0306234](#)].
- [21] A. Denner, S. Dittmaier, S. Kallweit, and A. Muck, *JHEP* **1203** (2012) 075, [[arXiv:1112.5142](#)].
- [22] O. Brein, A. Djouadi, and R. Harlander, *Phys.Lett.* **B579** (2004) 149–156, [[hep-ph/0307206](#)].
- [23] G. Ferrera, M. Grazzini, and F. Tramontano, *Phys.Rev.Lett.* **107** (2011) 152003, [[arXiv:1107.1164](#)].
- [24] M. Drees and K.-i. Hikasa, *Phys.Lett.* **B240** (1990) 455.
- [25] C. Anastasiou, F. Herzog, and A. Lazopoulos, *JHEP* **1203** (2012) 035, [[arXiv:1110.2368](#)].
- [26] O. Latunde-Dada *JHEP* **0905** (2009) 112, [[arXiv:0903.4135](#)].
- [27] S. Gieseke, D. Grellscheid, K. Hamilton, A. Papaefstathiou, S. Platzer, *et al.*, [arXiv:1102.1672](#).
- [28] K. Hamilton, P. Richardson, and J. Tully, *JHEP* **0904** (2009) 116, [[arXiv:0903.4345](#)].
- [29] A. Martin, W. Stirling, R. Thorne, and G. Watt, *Eur.Phys.J.* **C63** (2009) 189–285, [[arXiv:0901.0002](#)].
- [30] M. Whalley, D. Bourilkov, and R. Group, [hep-ph/0508110](#).
- [31] A. Djouadi, M. Spira, and P. Zerwas, *Z.Phys.* **C70** (1996) 427–434, [[hep-ph/9511344](#)].

- [32] A. Djouadi, J. Kalinowski, and M. Spira, *Comput.Phys.Commun.* **108** (1998) 56–74, [hep-ph/9704448].
- [33] LHC Higgs Cross Section Working Group, S. Dittmaier *et al.*, arXiv:1101.0593.
- [34] Y. L. Dokshitzer, G. Leder, S. Moretti, and B. Webber, *JHEP* **9708** (1997) 001, [hep-ph/9707323].
- [35] M. Wobisch and T. Wengler, hep-ph/9907280.
- [36] M. Cacciari, G. P. Salam, and G. Soyez, *Eur.Phys.J.* **C72** (2012) 1896, [arXiv:1111.6097].
- [37] M. Rubin *JHEP* **1005** (2010) 005, [arXiv:1002.4557].
- [38] A. Banfi, G. P. Salam, and G. Zanderighi, *JHEP* **0503** (2005) 073, [hep-ph/0407286].
- [39] A. Banfi, G. P. Salam, and G. Zanderighi, *JHEP* **1206** (2012) 159, [arXiv:1203.5773].
- [40] A. Banfi, P. F. Monni, G. P. Salam, and G. Zanderighi, arXiv:1206.4998.
- [41] T. Becher and M. Neubert, *JHEP* **1207** (2012) 108, [arXiv:1205.3806].
- [42] M. Klasen and G. Kramer, *Phys.Lett.* **B386** (1996) 384–388, [hep-ph/9605210].
- [43] S. Frixione and G. Ridolfi, *Nucl.Phys.* **B507** (1997) 315–333, [hep-ph/9707345].
- [44] A. Banfi and M. Dasgupta, *JHEP* **0401** (2004) 027, [hep-ph/0312108].
- [45] M. Cacciari, G. P. Salam, and G. Soyez, *JHEP* **0804** (2008) 063, [arXiv:0802.1189].
- [46] M. Dasgupta, L. Magnea, and G. P. Salam, *JHEP* **0802** (2008) 055, [arXiv:0712.3014].